PROCEEDINGS A

royalsocietypublishing.org/journal/rspa

Research

Cite this article: Frishman A, Grafke T. 2022 Mechanism for turbulence proliferation in subcritical flows. *Proc. R. Soc. A* **478**: 20220218. https://doi.org/10.1098/rspa.2022.0218

Received: 8 April 2022
Accepted: 6 September 2022

Subject Areas:
fluid mechanics, statistical physics

Keywords:
transitional turbulence, pipe flow, dynamical systems, stochastic transitions

Authors for correspondence:
Anna Frishman
e-mail: frishman@technion.ac.il
Tobias Grafke
e-mail: T.Grafke@warwick.ac.uk

Electronic supplementary material is available online at https://doi.org/10.6084/m9.figshare.c.6214729.

THE ROYAL SOCIETY PUBLISHING

Mechanism for turbulence proliferation in subcritical flows

Anna Frishman[1] and Tobias Grafke[2]

[1]Technion Israel Institute of Technology, 32000 Haifa, Israel
[2]University of Warwick, Coventry CV4 7AL, UK

AF, 0000-0003-1366-6293; TG, 0000-0003-0839-676X

The subcritical transition to turbulence, as occurs in pipe flow, is believed to generically be a phase transition in the directed percolation universality class. At its heart is a balance between the decay rate and proliferation rate of localized turbulent structures, called puffs in pipe flow. Here, we propose the first-ever dynamical mechanism for puff proliferation—the process by which a puff splits into two. In the first stage of our mechanism, a puff expands into a slug. In the second stage, a laminar gap is formed within the turbulent core. The notion of a split-edge state, mediating the transition from a single puff to a two-puff state, is introduced and its form is predicted. The role of fluctuations in the two stages of the transition, and how splits could be suppressed with increasing Reynolds number, are discussed. Using numerical simulations, the mechanism is validated within the stochastic Barkley model. Concrete predictions to test the proposed mechanism in pipe and other wall-bounded flows, and implications for the universality of the directed percolation picture, are discussed.

1. Introduction

How pipe flow becomes turbulent, a seemingly mundane phenomenon, has been a lasting puzzle for more than a century [1]. As first recognized by Reynolds, pipes have a transitional flow regime, where localized turbulent structures and laminar flow coexist [2–4]. However, a clear understanding of the nature of these structures, called puffs, and of the transition to turbulence with increasing Reynolds number Re, has only emerged in the past decade [5–7]. The current

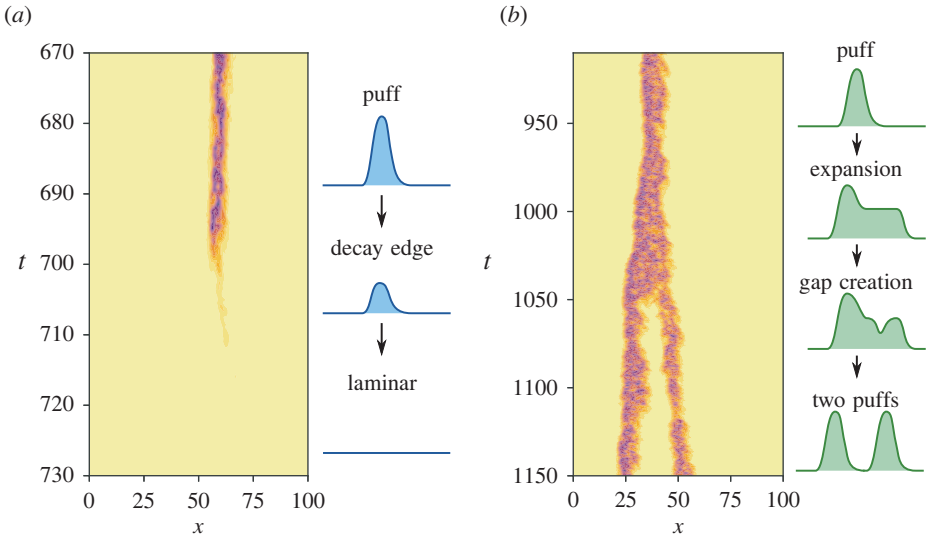

Figure 1. Illustration of puff decay and splitting mechanisms. (*a*) Decay mechanism—starting from a puff the system passes close to the decay edge before turning laminar. (*b*) Splitting mechanism—in the first stage, the puff expands into a slug with a turbulent core; in the second stage, a laminar gap is formed within the core. The trajectory passes close to the split edge. Trajectories are taken from the stochastic Barkley model. (Online version in colour.)

view is that it is an out-of equilibrium phase transition lying in the directed percolation universality class [8], and moreover that it is the ubiquitous route to turbulence for wall bounded flows.

For pipe flow, the extremely long time scales and length scales involved prevent a direct confirmation of this picture [9]. It has, however, been confirmed in other wall-bounded flows—which share much of the phenomenology of pipe flow [10,11], and where the critical point is more accessible [11–15].

Puffs are the basic degrees of freedom in the transitional picture. The fraction of the pipe occupied by puffs determines the level of turbulence, which is the order parameter for the transition. The absorbing state, required for a directed percolation transition, is the laminar flow: turbulent puffs cannot be spontaneously excited from it. The spatial proliferation of turbulence can thus only occur through puff splitting—a rare and random process by which two puffs are generated from a single puff. This process, however, competes with random decays of puffs, returning the flow back to the laminar state. The opposing tendencies with Re of these two processes bring about the critical point: decays become rarer with increasing Re, while splits become more frequent, with the critical point occurring roughly where the rates of the two balance [5,7].

The underlying dynamics controlling puff decays are relatively well understood, as sketched in figure 1*a*. They are driven by rare chaotic fluctuations which push the system across a phase space boundary between the laminar and puff state, the so-called edge of chaos [16–19]. On the way, the system passes close to a state which lies on this edge [20–23], here termed the *decay edge*, whose single unstable direction mediates the transition.

A comparable dynamical understanding of puff splitting is currently lacking. The directed percolation picture is predicated on splits becoming more frequent than decays with increasing Re; however, in the absence of a mechanism for puff splits, it remains unclear if that is the general rule and under what circumstances this type of transition could be absent. In this work, we propose the first-ever general mechanism for puff splitting and discuss how it can be suppressed. The mechanism, sketched in figure 1*b*, is a two-stage process: in the first stage, fluctuations drive a puff to expand through a structure called a slug. Slugs are observed at higher Re, where puffs are

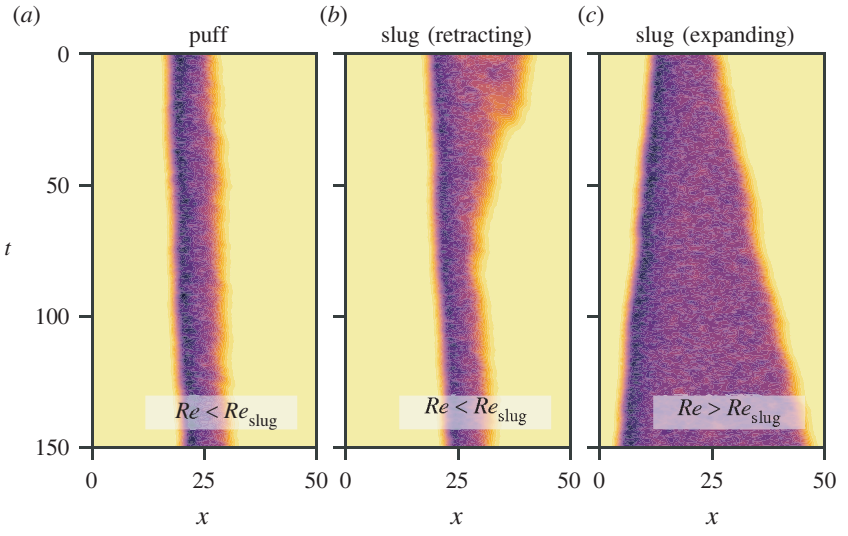

Figure 2. At $Re < Re_{slug}$, puffs are stable (*a*). For $Re > Re_{slug}$, turbulence expands via slugs (*c*). Slugs also exist for $Re < Re_{slug}$, but they retract into a puff instead of expanding (*b*). Realizations taken from the stochastic Barkley model. (Online version in colour.)

absent, and are similar to puffs except for their expanding core of homogeneous turbulence, see figure 2*c*. At the transitional *Re* we are considering here, we argue that such structures still exist and would contract as illustrated in figure 2*b*. To expand, they must be driven by rare fluctuations. In the second stage, when the slug is wide enough, a laminar pocket forms within the core, separating it into two parts, each of which evolves its own puff. We suggest that this transition is mediated by a state we call the *split edge*, lying at the boundary between a one-puff and a two-puff state. In the following, we motivate the viability of this picture for pipes and other wall-bounded flows sharing the same phenomenology. Some of the ingredients in our mechanism have not been directly observed in these flows; we explain why we believe they should be present. We validate the proposed mechanism within the stochastic Barkley model [6,7], presenting results taken from simulations, and leave a dedicated study of shear flows by direct numerical simulations to future work. Finally, we identify how the proposed split mechanism could be suppressed, discussing possible signatures.

2. The slug-gap-split mechanism

(a) Expansion stage

We begin by motivating a regime of *Re* where slugs and puffs coexist for pipe (and duct) flow. A slug is a structure interpolating in space between a homogeneous turbulent state at its core, where turbulence production balances turbulence dissipation, and laminar base flow at its sides. Slugs are observed at $Re > Re_{slug}$, where they replace puffs. It is also observed that the expansion rate of a slug grows continuously with *Re*, starting from zero at $Re = Re_{slug}$ [6,24]. We argue that this continuous transition implies that homogeneous turbulence can first be sustained at $Re < Re_{slug}$ (referred to as a masked transition in [6]), here denoted by Re_{turb}, see figure 3. Indeed, that the relative front speed for slugs continuously increases from zero at Re_{slug} implies that the transition from slugs to puffs with decreasing *Re* has to do with a change in front speed, rather than with the disappearance of homogeneous turbulence below Re_{slug}. If Re_{slug} was indeed the point where homogeneous turbulence is first sustained, one would not generically expect front speeds to match there.

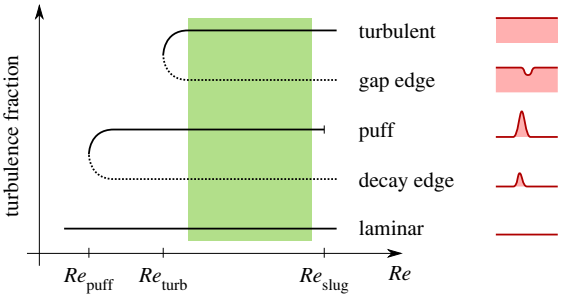

Figure 3. Bifurcation diagram (sketch) for transitional pipe flow. Green shaded region: applicability region of the proposed split mechanism. Attracting states are solid lines, unstable edge states are dotted. Right column: sketches of the corresponding states. In the deterministic Barkley model used here $r_{turb} = 0.667$ and $r_{slug} = 0.726$. (Online version in colour.)

Thus, slugs should be well defined dynamical states also in the range $Re_{turb} < Re < Re_{slug}$, developing when homogeneous turbulence and laminar flow are brought into spatial contact. The transition from slugs to puffs with decreasing Re is then a consequence of the expansion rate of a slug becoming negative in this range, as is consistent with a continuous decrease in relative front speed starting from zero at Re_{slug}. We thus expect that, once excited, a slug would contract and turn into a puff, as is illustrated in figure 2*b*. Such a contraction of slugs means that laminar flow overtakes homogeneous turbulence for this range of Re, implying that the turbulent state is metastable [8].

Note that we expect contracting slugs to be hard to observe in direct numerical simulations or experiments: chaotic fluctuations would quickly split a slug, through the mechanism explained below, if it is too wide. Indeed, contracting slugs have not been observed in shear flows to date. They are also hard to observe in the Barkley model for the classical parameters used in [7], where the noise level is much higher than the one we use in figure 2. However, if narrow enough, a contracting slug should be an observable dynamical state below Re_{slug}.

For the split mechanism, we propose that the most likely way to expand a puff is for random fluctuations to overcome the retraction of the slug. The first stage of our mechanism is thus the expansion of a puff, via rare chaotic fluctuations, into a slug with a wide enough turbulent core. This first stage is accessible at $Re_{turb} < Re < Re_{slug}$.

(b) Gap formation stage

The second stage corresponds to the transition from a slug with a turbulent core to a state with two puffs. For this stage, only the centre of the slug, namely its turbulent core, is relevant. Within this core, to end up with two separated puffs, a laminar gap must be formed by chaotic fluctuations.

When viewed locally, the creation of a laminar gap within turbulent flow is a transition in its own right. Namely from spatially homogeneous turbulence everywhere in the pipe, into a state with some laminar flow present. Indeed, homogeneous turbulence should be metastable for $Re < Re_{slug}$: a laminar-turbulent front would overtake the homogeneous turbulent flow, so that an opened laminar gap would expand and the state would not return to homogeneous turbulence. Along this transition, there should exist a minimal local perturbation of the homogeneous turbulence which will open a gap, and a corresponding mediating edge state: the *gap edge*, see figure 3.

We expect the gap edge to take the form of a local decrease of turbulence down to a threshold value. A further decrease of turbulence would widen the gap until laminar flow is formed, while an increase of turbulence would close it back. In that sense, the gap edge is the minimal nucleus of laminarity to create a lasting gap, mirroring the decay edge between laminar flow and a puff, which is the minimal nucleus of turbulence to create a turbulent puff.

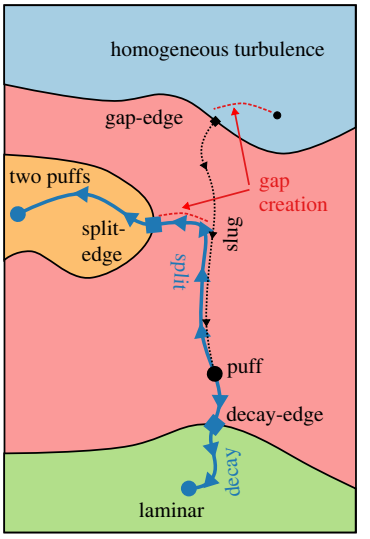

Figure 4. Sketch of the phase space, transitions and edge-states. From the puff basin (red region), the system can decay through the decay edge state into the laminar basin (green region). Alternatively, a puff can split, transitioning through the split edge state into the two puff basin (orange region). The split transition (blue line) consists of: (i) a slug driven by noise to expand, otherwise deterministically contracting (black dotted line), (ii) gap formation within the slug. This gap creation (red dotted) is the same as in the transition out of the homogeneous turbulence basin (blue region). (Online version in colour.)

The terminology *gap edge* implies that we expect this state to lie on a leaky basin boundary between two long-lived states. Indeed, for periodic boundary conditions, that would be the leaky boundary between a puff and a homogeneous turbulent state (which can thus be thought of as the edge of homogeneous chaos). Such a leaky boundary could form as a result of a boundary crisis, where the homogeneous turbulence state touches its basin boundary with the puff, making transitions to the puff state possible. A boundary crisis is also the mechanism believed to give rise to puff decays. Those are mediated by the decay edge, passing through the leaky boundary between the laminar and puff state [16,17]. From this point of view, a contracting slug is a dynamically favourable direction from the boundary between homogeneous turbulence and a puff, where the gap edge lies, to the puff see figure 4.

To summarize, we argue that after the expansion into a slug, the second stage on the way to a puff split is the above-described gap creation, occurring in the turbulent core of the slug.

(c) The split edge state

Viewed as a whole, the split transition requires crossing the boundary between one and two puffs, motivating yet another edge state—the *split edge*, see figure 4. Combining the two stages of the mechanism, the split edge should roughly take the form of a slug with a gap edge in its core, exactly wide enough to fit it, as sketched in figure 1. Indeed, local chaotic fluctuations of the gap edge along its unstable direction can either widen it, inducing a split, or close the gap, forming the core of a slug, which would then retract into a puff.

Here, we are suggesting the existence of a leaky boundary between a single puff and a two-puff state. Transitions from the two-puff state to a one-puff state are quite natural: they could occur through a decay of one of the puffs, implying an edge state of the form of a puff + decay edge. Such transitions would then be related to a boundary crisis where the two-puff state touches the boundary. However, such an edge state does not necessarily allow the opposite transition, from a single puff to two, since the decay edge cannot be spontaneously excited from laminar flow. Instead, we expect such transitions to be mediated by the proposed split-edge state,

corresponding to a boundary crisis where the two-puff state touches the boundary. This might explain the exponential distribution of transitions times from the one-puff to the two-puff state observed for puff splitting [5]. The leaky boundary between a one-puff and a two-puff state can thus include two embedded edge states, one for each direction. This complicates splitting events, since after reaching the two-puff basin, the system can recross the boundary back to a single puff state, giving rise to near-split events.

(d) Role of fluctuations

In the proposed mechanism, fluctuations have a double role: first, they drive the puff to become a slug and subsequently expand it. Second, when the core of the slug is wide enough to facilitate a gap edge, fluctuations drive the turbulence in the slug core below a threshold. It then generates an expanding laminar hole, with the two remaining segments of turbulence naturally evolving into puffs. Clearly, the expansion stage becomes more likely as Re increases, slugs contracting increasingly slower as Re_{slug} is approached. On the other hand, gap creation becomes less likely with increasing Re, since the homogeneous turbulent state becomes more stable. The latter trend is opposite to observations in straight pipes [5], implying that if our mechanism is at play, the gap creation is not the limiting factor in its splits. Finally note that the sustainment of the two-puff state at the end of the transition may also depend on fluctuations: the decay probability of the downstream puff is increased by close proximity to an upstream puff [7,25], causing near-split events [26] (electronic supplementary material).

3. Results for the Barkley model

In the remainder, we will demonstrate the relevance of the slug-gap-split mechanism focusing on transitional turbulence in the Barkley model. Each step of the analysis we perform could also be applied to direct numerical simulations of the Navier–Stokes equation, with appropriate adjustments. However, as it is significantly more computationally expensive to generate samples for the latter, here we limit the investigation to the Barkley model. This model is known to successfully reproduce both qualitative and quantitative features of pipe and duct flow [6], relying on minimal modelling ingredients. Moreover, in the presence of stochastic noise, the model also goes through a directed percolation transition, facilitated by puff decays and splits [7]. Note that the deterministic Barkley model does not exhibit chaos nor proper turbulence, but rather captures the underlying phase space structure. In particular, puffs and homogeneous turbulence are deterministic states in the model. Transitions between basins of attraction are then made possible by the inclusion of the noise, which models chaotic fluctuations and allows for leaky boundaries.

The model is one-dimensional, describing the coarse-grained dynamics along the pipe direction x, and employs two variables: the mean shear $u(x,t)$ and turbulent velocity fluctuations $q(x,t)$ [27]. Alternatively, $u(x,t)$ can be interpreted as the local centerline velocity, which becomes smaller in the presence of turbulence—namely dropping down to the mean flow rate $\bar{U}$, and is largest for laminar flow at U_0.

The Barkley model is given by

$$\begin{cases} \partial_t q + (u-\zeta)\partial_x q = f_r(q,u) + D\partial_x^2 q + \sigma q\eta \\ \partial_t u + u\partial_x u = \epsilon[(U_0-u) + \kappa(\bar{U}-u)q], \end{cases} \tag{3.1}$$

where $f_r(q,u) = q(r+u-U_0-(r+\delta)(q-1)^2)$. The parameter r is the most important, and plays the role of Re. The parameter D controls the strength of turbulence diffusion, ϵ the (slow) relaxation of the mean flow to the base laminar profile, κ the influence of turbulence on the mean flow profile (blunting it), and δ provides a finite threshold keeping the laminar base flow stable in the limit $r \to \infty$. Lastly, η is a spatio-temporal white noise with amplitude σ. It is multiplicative to mimic the proportionality of chaotic fluctuations in actual flow to the turbulence level present at

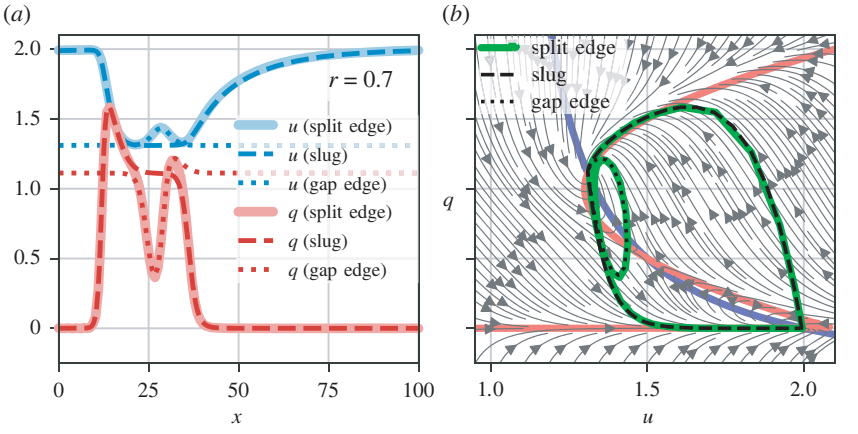

Figure 5. Deterministic edge state between one and two puffs, the *split edge* (solid), overlaid are a slug (dashed) and a gap edge (dotted). Configurations are shown in space (*a*) and in the *u*-*q*-plane (*b*). (Online version in colour.)

that point (importantly, turbulence cannot be excited from laminar flow where $q = 0$). The values of parameters we choose for our numerical experiments is discussed in §5. The Barkley model has been demonstrated to quantitatively capture features of transitional pipe flow remarkably well [6,7].

In the model, the base laminar flow and homogeneous turbulent state (as is present in the core of the slug) are fixed points: $q = 0, u = U_0$ and (q_t, u_t) correspondingly. Our focus is the range $r_{\mathrm{turb}} < r < r_{\mathrm{slug}}$ where the turbulent fixed point coexists with puffs. As sketched in figure 3, in the model the turbulent fixed point appears in a saddle node bifurcation at $r = r_{\mathrm{turb}}$ together with an unstable travelling wave—the gap edge state described above. See [28] for a full classification of states.

Before turning to stochastic transitions, we analyse the split edge state lying at the boundary between a one-puff and a two-puff state. We locate the split edge state using edge tracking within the deterministic model. Spatial profiles of q, u for the split edge are shown in figure 5*a*. To confirm the proposed mechanism is at play, we have also obtained the gap edge for the model via edge tracking. Superposing the gap edge and a slug with a (momentarily) equal spatial extent onto the split edge indeed gives an almost exact match. This match between the three objects is also shown in a plot in the *q*-*u*-plane in figure 5*b*.

4. Stochastic transitions in the Barkley model

Decay and split transitions are made possible via random fluctuations—chaotic in pipe flow and stochastic in the Barkley model—whose rare realizations bring them about. These transitions are thus probabilistic in nature, and so must be the comparison to an underlying dynamical mechanism. We first demonstrate our method of analysis and the required probabilistic notions for decay transitions, which are simpler in nature and are already well understood. We then apply these ideas to test the slug-gap-split mechanism.

(a) Puff decay

We set out to confirm that the decay transition is a trajectory connecting the puff state to the laminar state, crossing the boundary through the decay edge. To that end, we collect many decay trajectories in the stochastic Barkley model. The average decay path is shown in figure 6 as a space–time plot of the average value of q along the transition. It is presented in the frame of reference moving at the average speed of a puff. A visual signature that the trajectory goes

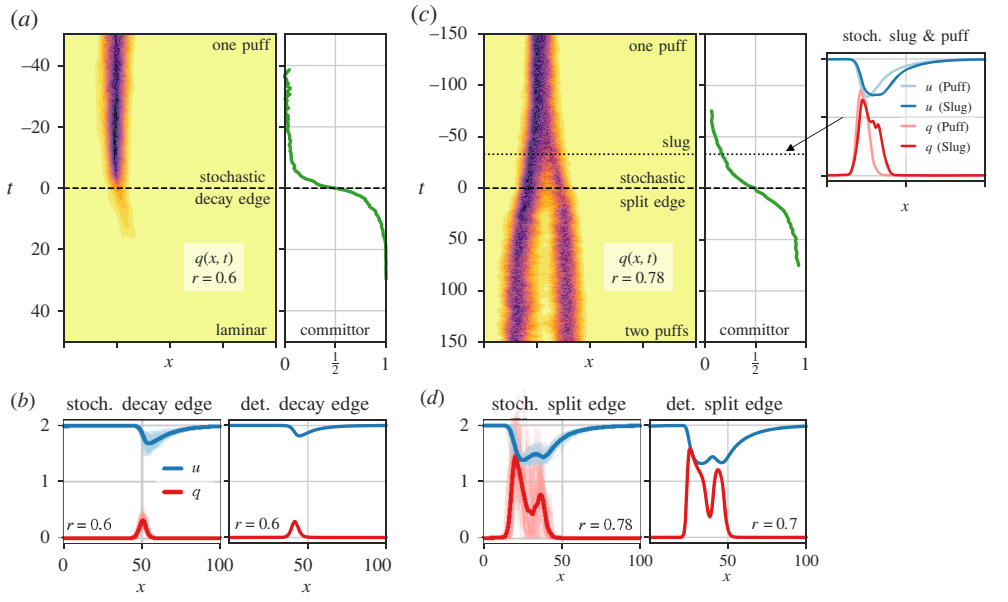

Figure 6. Transitions in the puff regime, $r_{\text{turb}} < r < r_{\text{slug}}$ in the Barkley model where r is a proxy for Re. (*a*) Left: $q(x, t)$ of the average stochastic decay trajectory in space–time. Right: average committor along the transition. (*b*) Left: average stochastic decay edge, corresponding to the dashed line in (*a*), on top of individual realizations in transparent colour. Right: deterministic decay edge. (*c*) Left: average stochastic split trajectory. Right: average committor. Inset: average spatial profile at an initial stage of the transition, having a slug-like structure, along with an average puff. (*d*) Left: average stochastic split edge, on top of individual realizations. Right: deterministic split edge.

through the decay edge is the increase in speed during the decay, the decay edge moving at a speed $\approx U_0 - \zeta$ [7,22,24].

In order to speak about an edge between different states in noisy, stochastic datasets, we further introduce the notion of the *stochastic decay edge*: this is the set of configurations with the property of having an equal probability to transition to laminar flow or to become a puff. Since all observed decay events happen in a very similar manner, the average of these stochastic decay edge states is a meaningful state itself. Specifically, we obtain the stochastic edge in the following way: given an observed decay trajectory we initiate many stochastic simulations from configurations along it, and measure the likelihood of continuing on the transition. This defines the *committor* for the given trajectory (see §5). We then identify the configuration from which there is an equal probability to transition or return back, i.e. where the value of the committor is 1/2. Repeating this for many decay trajectories yields the set of configurations defining the stochastic edge.

We expect the average stochastic edge state to be similar in structure to the deterministic decay edge. This is confirmed in our numerical experiments. Figure 6*b* (left) shows the spatial profiles of the average stochastic decay edge, averaged over the different trajectories, on top of individual realizations. For comparison, a deterministic decay edge is shown in figure 6*b* (right). In figure 6*a*, we show the average transition path alongside the committor, averaged over decay trajectories. Examples of the committor for individual trajectories are presented in the electronic supplementary material.

(b) Puff splitting

We can now apply these same ideas to the puff splitting transition. Concretely, to test the relevance of the slug-gap-split mechanism to stochastic transitions in the Barkley model, we will use the average transition path obtained from random puff splits. In figure 6*c*, we present this average

path, where trajectories are aligned according to the location of the stochastic split edge. The latter is obtained using the same algorithm as for the stochastic decay edge; the corresponding average committor is shown in figure 6*c*. Note the striking resemblance of the average transition to a single realization of a band split in channel flow in a narrow domain [26,29]. The average transition presented in figure 6*c* indeed reflects the typical splitting trajectory in the Barkley model, such as that in figure 1*b*; outliers were included in the averaging but had a negligible effect. Examples of outlier splitting trajectories are shown in the electronic supplementary material.

The average transition path clearly shows the expansion stage of the slug-gap-split mechanism: as seen in the inset of figure 6*c*, prior to the creation of the laminar hole the puff extends into a wider turbulent structure. Moreover, this average structure resembles a slug, containing a small homogeneous region most clearly seen in the u profile. Furthermore, the structure always has the same spatial extent right before gap formation, indicating an expansion stage up to the necessary length. To test the gap formation stage, we now compare the average stochastic split edge state to the deterministic split edge. The stochastic split edge is presented in figure 6*d* (left) on top of individual realizations, while the deterministic edge is shown figure 6*d* (right). There is very good qualitative agreement between the two. Note that the stochastic noise induces parameter shifts, e.g. of r_{slug}, compared with the deterministic model [7] (electronic supplementary material); thus we keep the comparison qualitative.

For the parameters used here, we observe that the main bottleneck for the transition is the first stage, expansion of the slug. Indeed, once the slug is wide enough, a laminar gap is likely to form, which smears the gap within the stochastic split edge in figure 6*d* (left). The likelihood of splits is thus dominated by the expansion stage, whose likelihood increases with r, as is consistent with observations for the model.

5. Methodology for the Barkley model analysis

In the following, we will describe the numerical algorithms we implemented in order to obtain critical points of the dynamics (i.e. stable fixed points and edge states), as well as the methodology used to obtain information about the stochastic transition, the ensemble of transition trajectories, the committor function, and the stochastic edge state.

(a) Stable states

In order to find the stable states (turbulent, puff, laminar) of the Barkley model, we numerically integrate it with parameters $\zeta = 0.8$, $\delta = 0.1$, $\epsilon = 0.1$, $\kappa = 2$, $U_0 = 2$, $\bar{U} = 1$ and $D = 0.5$, additionally with small diffusion coefficient for the velocity $D_u = 10^{-2}$ which is not expected to affect the results [7]. The noise amplitude σ is $\sigma = 0$ for deterministic simulations and $\sigma = 0.5$ for stochastic simulations, except in figure 2 where $\sigma = 0.2$ for demonstration purposes. All numerical simulations are performed in a periodic spatial domain $x \in [0, L]$, with $L = 100$.

The functions $q(x)$ and $u(x)$ are discretized on an equidistant computational grid with $N_x = 128$ or $N_x = 256$ grid points. Spatial derivatives are computed pseudo-spectrally, by using the fast Fourier-transform. We use exponential time differencing (ETD) [30] as a temporal integrator, which is exact for all linear terms, and first order for the nonlinear (reaction) terms. The time-step is chosen between $\Delta t = 10^{-2}$ and $\Delta t = 10^{-3}$. In order to include stochasticity, we generalize first-order ETD to include the stochastic increment, similar to [31,32].

The puff, gap edge and split edge are travelling at fixed speed along the pipe, and are therefore not proper fixed points but instead limit cycles of the dynamics. We fix for that by transforming into a moving reference frame adaptively, so that the centre of turbulent mass of the objects remains stationary.

(b) Edge tracking algorithm

To find the *unstable* fixed points, i.e. the edge states between puff and laminar flow (the decay edge), between puff and two puffs (the split edge) and between turbulent flow and puff (the gap edge), we employ edge tracking. This algorithm integrates forward in time two copies of the system, one in each basin of attraction between which the edge state is to be found. The two copies are kept close via a bisection procedure to converge back to the separating manifold should the states drift too far apart. Effectively, this procedure integrates the system's dynamics, but restricted to the separating manifold between two stable states. The individual fixed points (laminar, puff, turbulent, two puffs) are identified via their turbulent mass $\bar{q} = \int_0^L q(x)\,dx$.

(c) Stochastic transitions

(i) Ensemble of transition trajectories

Including stochasticity into the Barkley model, $\sigma \neq 0$, allows the model to *transition* between different metastable states. For example, the puff state is always coexistent with the laminar state, and fluctuations can drive the puff into eventual decay. Numerically, we generate an ensemble of transitions between two states by initializing in one state, and then simulating the stochastic dynamics until another state is observed.

For decays, we identify whether a configuration has entered the laminar state or the turbulent state by checking whether its turbulent mass $\bar{q}$ is within an interval of the expected turbulent mass of the laminar state $\bar{q} = 0$ or the turbulent state $\bar{q} = q_t$. For the one puff state, we similarly compare the configuration's turbulent mass to that of the average puff. It is less straightforward to identify the two-puff state. Here, we flag a potential puff split event if the fifth Fourier-mode of q exceeds a threshold, which for our parameters was empirically identified to be sensitive to the formation of a gap. Whether a split has indeed taken place is then later checked when computing the committor along the transition and seeing whether it ever reaches one; see §ii. This way, we avoid flagging 'near-split' events, where a turbulent region separates from the main puff, but is too small to eventually survive.

(ii) Stochastic edge tracking

In order to compare edge states between the deterministic model (where edge states can be exactly found, but transitions never happen), and the stochastic model (where noise-induced transitions can be observed, but fixed points can only be identified on average), we develop the notion of the *stochastic edge*. The underlying intuition comes from the forward committor function known in transition path theory [33,34]: given a stochastic process X_t on some state space Ω, consider two subsets $A \subset \Omega$ the reactant state, and $B \subset \Omega$ the product state. We are interested in transitions of the process from A to B. The (forward) committor $p^+ : \Omega \mapsto [0, 1]$ for the transition $A \to B$ denotes the probability that the process visits B next, before visiting A. Intuitively, the committor measures how much the system is 'committed' to performing the transition. While the committor can be precisely defined for both stochastic and deterministic processes [34], its computation through solving a Fokker–Planck type equation is prohobitive for any large system. Instead, for stochastic systems such as the Barkley model, the committor can be estimated by sampling many realizations of the process and counting the occurrences of the transition event.

After generating an ensemble of transitions between two attractors as described above in §i, we can set out to numerically compute the committor along these transition trajectories. One can numerically find the committor of a configuration (q, u) via sampling: initialize the simulation at (q, u) and sample many times, measuring whether we visit the product state before the reactant state. We do so for many states along each individual transition trajectory. For example, for a stochastic transition between the puff and laminar flow, close to the puff the committor will be almost zero. Close to the laminar state, the committor will be almost one. In between, there is a region where the committor takes intermediate values. We define the *stochastic edge* of a transition

to be a state at which the committor takes the value $\frac{1}{2}$. Note that for a stochastic transition a committor value of $\frac{1}{2}$ can be attained multiple times per transition. In our case, we pick as the relevant stochastic edge the state where the committor is closest to $\frac{1}{2}$ throughout the transition, and take the first such state if there are several.

In practice, for the puff decay transition, we define both the set A, the puff, and the set B, the laminar state, by thresholding its turbulent mass $\bar{q}$. For the puff split transition, we define the set A, the one puff state, and the set B, the two puff state, by thresholding the second cumulant under q, i.e. $\langle x^2\rangle_q - \langle x\rangle_q^2$. This quantity measures to what degree turbulent mass is distributed away from the centre of turbulent mass, $\langle x\rangle_q$. It is therefore small for the localized one-puff state, but large for the two-puff state, where the centre of mass is located somewhere between the two puffs. The quantity is also large for extended slugs without a gap which might occur during a transition event. To avoid mis-identifying a slug for two puffs, we check the threshold criterion for a prolonged time interval. If the configuration remains above the threshold very long, then it is almost guaranteed to be in the (long lived, stationary) two-puff state, instead of the (short-lived, transient) extended slug state or other mixed states, which quickly decay.

(iii) Averaged stochastic transition path

In order to obtain an average stochastic transition path, we average all individual trajectories of our ensemble of transition trajectories obtained as described in (i). We average the committor of individual trajectories over the ensemble of transition trajectories, by aligning in time the numerically measured committor at the stochastic edge. Note, though, that the average committor is not identical to the committor of the average transition trajectory. We nevertheless show the average committor to give an impression of how fast the transition happens: the sharpness of the transition from 0 to 1 indicates the time scale of the transition itself.

6. Conclusion and discussion

The subcritical transition to turbulence is generically characterized by the appearance of localized turbulent patches, called puffs in pipe flow, whose proliferation brings about a sustained turbulent phase. Here, we have presented the first detailed proposal for the dynamics underlying the proliferation process: a dynamical puff-splitting mechanism termed the slug-gap-split mechanism. We have motivated the relevance of this mechanism for pipe flow, and confirmed its presence in the Barkley model. The proposed slug-gap-split mechanism implies concrete predictions, making the proposal testable. Moreover, it introduces a novel framework within which previous observations could be interpreted, and alternatives for other wall-bounded flows could be explored. We now discuss these issues in detail.

Previously, splitting had been observed to occur through the following process [5,9,35]: the puff continuously emits vortices (turbulence) from its downstream edge, then, if this patch of vortices manages to persist and sufficiently separates from the parent puff, it seeds a new puff. These observations could be consistent with the slug-gap-split mechanism, with the growth of the daughter puff occurring after the crossing of the phase space boundary between a single puff and two. The possible subsequent decay would then correspond to a near-split event, a recrossing of this boundary. Still, such observations could also imply that a different mechanism is at play, whereby a puff emits a turbulent patch without going through an expansion stage first. An expansion stage where a small core of balanced turbulence forms within the puff is thus a distinct prediction of the slug-gap-split mechanism. Only then does a laminar gap appear in this picture, and the structure evolves towards two puffs. The latter process can then sometimes fail if the downstream puff is snuffed out by the upstream one. It is worth noting that the splitting process looks much less symmetric in pipe flow compared to that in the Barkley model. That, however, might be a visual artefact: the Barkley model does not capture the very steep increase in turbulence level observed at an upstream front, making the puff appear more symmetric and thus

also the splitting process.[1] This quantitative feature should not influence the applicability of the slug-gap-split mechanism, which does not rely on it. In fact, the results presented in [35] for the centerline velocity during a split in pipe flow do seem to indicate a split through the formation of a laminar gap within turbulent flow, though further study is needed.

To distinguish between the different mechanisms that could be at play for splits, the analysis outlined above for the Barkley model could be carried out in direct numerical simulations. First, the split edge state could be located using edge tracking, as previously done for the decay edge state [20,22,24]. Second, a probabilistic analysis of split transitions using the committor between one and two puffs, akin to the one introduced here, could also be carried out. It would reveal the average transition path and the stochastic edge state, which could be compared with the expectations from the slug-gap-split mechanism. Note that the stochastic edge state, defined here directly via transitional trajectories, is not *a priori* identical to the split edge state found via edge tracking. The comparison between the two would test the role played by the latter in the transitions.

The slug-gap-split mechanism is restricted to the range $Re_{\mathrm{turb}} < Re < Re_{\mathrm{slug}}$. This suggests a novel possibility that more than a single splitting mechanism exists, and that different mechanisms could dominate at different Re. It would thus be interesting to assess Re_{turb} for pipe flow, e.g. using a minimal flow unit [36,37], and comparing it to the Reynolds number at the directed percolation critical point. Indeed, while we expect our mechanism to dominate close to Re_{slug}, it is not guaranteed to survive down to the critical point. At lower Re it could in principle be replaced by a process whereby a puff emits a turbulent patch, as described above. The split edge state would then take a different character (electronic supplementary material).

While we have focused on pipe flow so far, other wall-bounded flows which exhibit a subcritical transition to turbulence (and have a single extended direction) are captured within the same framework. Indeed, splits in Couette and channel flow in a narrow domain seem to follow the proposed mechanism: an expansion stage is observed, followed by the formation of a laminar gap [12,26,29]. Generally, the key condition for the slug-gap-split mechanism to be relevant is for the expansion rate of turbulence to continuously increase with Re, starting from zero at the transition from puffs to slugs.

Our work offers a novel point of view on how the phenomenology of other wall-bounded flows could differ from that of pipe flow. In particular, we now discuss a mechanism by which splits could be suppressed compared to decays, and therefore a directed-percolation-type transition would be impossible. This could be relevant for slightly bent pipes [38,39]. In the slug-gap-split mechanism, the likelihood of the transition is the multiplication of that of the expansion stage, which increases with Re, and of the gap creation stage, which decreases with Re. If the latter is sufficiently high close to Re_{slug} then transitions would become more likely with Re, as observed in pipes. However, splitting could be limited by gap creation if such creation becomes improbable at a sufficiently low Re. Then, splits would become less likely with increasing Re and would be most difficult to observe close to Re_{slug}. The occurrence of a directed percolation critical point requires that the probability of puff splitting roughly balances that of puff decay. Such a balance is not guaranteed if, for large enough Reynolds numbers, both decays and splits become increasingly improbable with Re. Splits could then remain less probable than decays for the entire range of Re.

A signature that gap creation is indeed a limiting factor for puff splits would be the absence of an intermittent turbulent regime above Re_{slug}. This regime, observed in pipe flow [40], is characterized by laminar gaps randomly opening within the homogeneous turbulent state, persisting and randomly closing. Indeed, if reaching the gap edge is prohibitively improbable for splits, such laminar gap excitations would also be suppressed [28]. In fact, such a correlation seems to exist for slightly bent pipes [38], providing a tantalizing connection to the suggested scenario.

[1]Indeed, when the turbulence level at the upstream front is accentuated for the Barkley model, as done in [7], splits in the Barkley model look very similar to those in pipe flow

Data accessibility. All data used to perform this study and the code to generate the presented figures are made available.

The data are provided in the electronic supplementary material [41].

Authors' contributions. A.F.: conceptualization, formal analysis, methodology, writing—original draft, writing—review and editing; T.G.: conceptualization, formal analysis, methodology, software, visualization, writing—original draft, writing—review and editing.

Both authors gave final approval for publication and agreed to be held accountable for the work performed therein.

Conflict of interest declaration. We declare we have no competing interests.

Funding. T.G. acknowledges support from EPSRC projects EP/T011866/1 and EP/V013319/1.

Acknowledgements. We thank Dwight Barkley, Sébastien Gomé and Laurette Tuckerman for helpful discussions and comments. We are additionally grateful for input from Yariv Kafri, Dov Levine and Grisha Falkovich.

References

1. Reynolds O. 1883 An experimental investigation of the circumstances which determine whether the motion of water shall be direct or sinuous, and of the law of resistance in parallel channels. *Proc. R. Soc.* **35**, 935–982. (doi:10.1098/rstl.1883.0029)
2. Lindgren ER. 1957 The transition process and other phenomena in viscous flow. *Arkiv fysik* 12.
3. Wygnanski IJ, Champagne F. 1973 On transition in a pipe. Part 1. The origin of puffs and slugs and the flow in a turbulent slug. *J. Fluid Mech.* **59**, 281–335. (doi:10.1017/S0022112073001576)
4. Darbyshire AG, Mullin T. 1995 Transition to turbulence in constant-mass-flux pipe flow. *J. Fluid Mech.* **289**, 83–114. (doi:10.1017/S0022112095001248)
5. Avila K, Moxey D, de Lozar A, Avila M, Barkley D, Hof B. 2011 The onset of turbulence in pipe flow. *Science* **333**, 192–196. (doi:10.1126/science.1203223)
6. Barkley D, Song B, Mukund V, Lemoult G, Avila M, Hof B. 2015 The rise of fully turbulent flow. *Nature* **526**, 550–553. (doi:10.1038/nature15701)
7. Barkley D. 2016 Theoretical perspective on the route to turbulence in a pipe. *J. Fluid Mech.* **803**, 1. (doi:10.1017/jfm.2016.465)
8. Pomeau Y. 1986 Front motion, metastability and subcritical bifurcations in hydrodynamics. *Physica D* **23**, 3–11. (doi:10.1016/0167-2789(86)90104-1)
9. Mukund V, Hof B. 2018 The critical point of the transition to turbulence in pipe flow. *J. Fluid Mech.* **839**, 76–94. (doi:10.1017/jfm.2017.923)
10. Manneville P. 2016 Transition to turbulence in wall-bounded flows: where do we stand? *Mech. Eng. Rev.* **3**, 15–00684–15–00684. (doi:10.1299/mer.15-00684)
11. Tuckerman LS, Chantry M, Barkley D. 2020 Patterns in wall-bounded shear flows. *Annu. Rev. Fluid Mech.* **52**, 343–367. (doi:10.1146/annurev-fluid-010719-060221)
12. Shi L, Avila M, Hof B. 2013 Scale invariance at the onset of turbulence in Couette flow. *Phys. Rev. Lett.* **110**, 204502. (doi:10.1103/PhysRevLett.110.204502)
13. Lemoult G, Shi L, Avila K, Jalikop SV, Avila M, Hof B. 2016 Directed percolation phase transition to sustained turbulence in Couette flow. *Nat. Phys.* **12**, 254–258. (doi:10.1038/nphys3675)
14. Chantry M, Tuckerman LS, Barkley D. 2017 Universal continuous transition to turbulence in a planar shear flow. *J. Fluid Mech.* **824**, R1. (doi:10.1017/jfm.2017.405)
15. Klotz L, Lemoult G, Avila K, Hof B. 2022 Phase transition to turbulence in spatially extended shear flows. *Phys. Rev. Lett.* **128**, 014502. (doi:10.1103/PhysRevLett.128.014502)
16. Skufca JD, Yorke JA, Eckhardt B. 2006 Edge of chaos in a parallel shear flow. *Phys. Rev. Lett.* **96**, 174101. (doi:10.1103/PhysRevLett.96.174101)
17. de Lozar A, Mellibovsky F, Avila M, Hof B. 2012 Edge state in pipe flow experiments. *Phys. Rev. Lett.* **108**, 214502. (doi:10.1103/PhysRevLett.108.214502)
18. Budanur NB, Dogra AS, Hof B. 2019 Geometry of transient chaos in streamwise-localized pipe flow turbulence. *Phys. Rev. Fluids* **4**, 102401. (doi:10.1103/PhysRevFluids.4.102401)
19. Rolland J. 2018 Extremely rare collapse and build-up of turbulence in stochastic models of transitional wall flows. *Phys. Rev. E* **97**, 023109. (doi:10.1103/PhysRevE.97.023109)
20. Schneider TM, Eckhardt B, Yorke JA. 2007 Turbulence transition and the edge of chaos in pipe flow. *Phys. Rev. Lett.* **99**, 034502. (doi:10.1103/PhysRevLett.99.034502)
21. Duguet Y, Willis AP, KerswellL RR. 2008 Transition in pipe flow: the saddle structure on the boundary of turbulence. *J. Fluid Mech.* **613**, 255–274. (doi:10.1017/S0022112008003248)

22. Mellibovsky F, Meseguer A, Schneider TM, Eckhardt B. 2009 Transition in localized pipe flow turbulence. *Phys. Rev. Lett.* **103**, 054502. (doi:10.1103/PhysRevLett.103.054502)
23. Avila M, Mellibovsky F, Roland N, Hof B. 2013 Streamwise-localized solutions at the onset of turbulence in pipe flow. *Phys. Rev. Lett.* **110**, 224502. (doi:10.1103/PhysRevLett.110.224502)
24. Duguet Y, Willis AP, Kerswell RR. 2010 Slug genesis in cylindrical pipe flow. *J. Fluid Mech.* **663**, 180–208. (doi:10.1017/S0022112010003435)
25. Hof B, De Lozar A, Avila M, Tu X, Schneider TM. 2010 Eliminating turbulence in spatially intermittent flows. *Science* **327**, 1491–1494. (doi:10.1126/science.1186091)
26. Gomé S, Tuckerman LS, Barkley D. 2021 Extreme events in transitional turbulence. (http://arxiv.org/abs/2109.01476).
27. Song B, Barkley D, Hof B, Avila M. 2017 Speed and structure of turbulent fronts in pipe flow. *J. Fluid Mech.* **813**, 1045–1059. (doi:10.1017/jfm.2017.14)
28. Anna F, Tobias G. 2022 The dynamical landscape of transitional pipe flow.
29. Gomé S, Tuckerman LS, Barkley D. 2020 Statistical transition to turbulence in plane channel flow. *Phys. Rev. Fluids* **5**, 083905. (doi:10.1103/PhysRevFluids.5.083905)
30. Cox S, Matthews P. 2002 Exponential time differencing for stiff systems. *J. Comput. Phys.* **176**, 430–455. (doi:10.1006/jcph.2002.6995)
31. Kloeden PE, Lord GJ, Neuenkirch A, Shardlow T. 2011 The exponential integrator scheme for stochastic partial differential equations: pathwise error bounds. *J. Comput. Appl. Math.* **235**, 1245–1260. (doi:10.1016/j.cam.2010.08.011)
32. Lord GJ, Tambue A. 2013 Stochastic exponential integrators for the finite element discretization of SPDEs for multiplicative and additive noise. *IMA J. Numer. Anal.* **33**, 515–543. (doi:10.1093/imanum/drr059)
33. Vanden-Eijnden E. 2006 Transition path theory. In *Computer Simulations in Condensed Matter Systems: From Materials to Chemical Biology* (eds M Ferrario, G Ciccotti, K Binder), vol. 1, Lecture Notes in Physics, pp. 453–493. Berlin, Heidelberg: Springer.
34. Weinan E, Vanden-Eijnden E. 2010 Transition-path theory and path-finding algorithms for the study of rare events. *Annu. Rev. Phys. Chem.* **61**, 391–420. (doi:10.1146/annurev.physchem.040808.090412)
35. Shimizu M, Manneville P, Duguet Y, Kawahara G. 2014 Splitting of a turbulent puff in pipe flow. *Fluid Dyn. Res.* **46**, 061403. (doi:10.1088/0169-5983/46/6/061403)
36. Jiménez J, Moin P. 1991 The minimal flow unit in near-wall turbulence. *J. Fluid Mech.* **225**, 213–240. (doi:10.1017/S0022112091002033)
37. Hamilton JM, Kim J, Waleffe F. 1995 Regeneration mechanisms of near-wall turbulence structures. *J. Fluid Mech.* **287**, 317–348. (doi:10.1017/S0022112095000978)
38. Rinaldi E, Canton J, Schlatter P. 2019 The vanishing of strong turbulent fronts in bent pipes. *J. Fluid Mech.* **866**, 487–502. (doi:10.1017/jfm.2019.120)
39. Barkley D. 2019 Taming turbulent fronts by bending pipes. *J. Fluid Mech.* **872**, 1–4. (doi:10.1017/jfm.2019.340)
40. Moxey D, Barkley D. 2010 Distinct large-scale turbulent-laminar states in transitional pipe flow. *Proc. Natl Acad. Sci. USA* **107**, 8091–8096. (doi:10.1073/pnas.0909560107)
41. Frishman A, Grafke T. 2022 Mechanism for turbulence proliferation in subcritical flows. Figshare. (doi:10.6084/m9.figshare.c.6214729)